The 7.5-Å Electron Density and Spectroscopic Properties of a Novel Low-Light B800 LH2 from *Rhodopseudomonas palustris*

Nichola Hartigan, Hazel A. Tharia, Frank Sweeney, Anna M. Lawless, and Miroslav Z. Papiz
Department of Synchrotron Radiation, CLRC Daresbury Laboratory, Warrington, Cheshire WA4 4AD, United Kingdom

ABSTRACT A novel low-light (LL) adapted light-harvesting complex II has been isolated from *Rhodopseudomonas palustris.* Previous work has identified a LL B800–850 complex with a heterogeneous peptide composition and reduced absorption at 850 nm. The work presented here shows the 850 nm absorption to be contamination from a high-light B800–850 complex and that the true LL light-harvesting complex II is a novel B800 complex composed of eight $\alpha\beta_d$ peptide pairs that exhibits unique absorption and circular dichroism near infrared spectra. Biochemical analysis shows there to be four bacteriochlorophyll molecules per $\alpha\beta$ peptide rather than the usual three. The electron density of the complex at 7.5 Å resolution shows it to be an octamer with exact 8-fold rotational symmetry. A number of bacteriochlorophyll geometries have been investigated by simulation of the circular dichroism and absorption spectra and compared, for consistency, with the electron density. Modeling of the spectra suggests that the B850 bacteriochlorophylls may be arranged in a radial direction rather than the usual tangential arrangement found in B800–850 complexes.

INTRODUCTION

Photosynthetic light-harvesting (LH) complexes are produced in the intracytoplasmic membranes of purple bacteria and have been the subject of intensive research in recent years. The structure of LH1 complex from *Rhodospirillum rubrum* has been determined at 8.5 Å resolution by cryo-electron microscopy (Karrasch et al., 1995). The peripheral LH2 structures from *Rhodopseudomonas acidophila* (McDermott et al., 1995) and *Rhodospirillum molischianum* (Koepke et al., 1996) have been determined at high resolution by single crystal x-ray diffraction. LH complexes are cyclical arrangements of peptides and pigments: 16 units for LH1 of *Rs. rubrum*, 9 for LH2 of *Rps. acidophila*, and 8 for LH2 of *Rs. molischianum*. Knowledge of the three-dimensional arrangement of pigments within these structures has allowed the correlation of their structural and spectroscopic properties. A key question is: to what extent is the absorbed energy delocalized among the red-most absorbing components of the bacteriochlorophyll (Bchl *a*) pigments that mediate energy transfer between the complexes (Nagarajan et al., 1996; Jimenez et al., 1996; Pullerits et al., 1996; Leegwater, 1996; Sundström et al., 1999)? A number of spectroscopic experiments have been interpreted as showing delocalization over anywhere between two and all of the B850/B880 molecules responsible for the long wavelength absorption (Pullerits et al., 1996; Chachisvilis et al., 1997; Monshouwer et al., 1997; Nagarajan et al., 1996; Meier et al., 1997; Leupold et al., 1996; Jimenez et al., 1997; Novoderezhkin et al., 1999).

The functionally active components of LH complexes are Bchl *a* and carotenoid molecules. Carotenoids absorb in the visible part of the spectrum and are responsible for the characteristic colors of LH complexes. It is the Bchl *a* Qy transition dipole moments, in the near infrared (NIR) region between 800 and 890 nm, that are involved in energy transfer between complexes. LH2 complexes are more numerous and varied in spectral type than LH1 complexes, and in some purple bacteria, a number of LH2 complexes are expressed under different conditions of light and temperature (Hawthornthwaite and Cogdell, 1991; Zuber and Brunisholz, 1991). In most species, LH1 complexes seem to absorb as a single NIR peak located between 875 and 890 nm whereas LH2 complexes show two distinct bands; one at 800 nm and another between 820 and 860 nm. Typically, there are two types of LH2 complexes, B800–820 and B800–850. The naming of these complexes is a convention that groups structurally and spectroscopically similar types of LH complexes and does not imply exact wavelength values.

In B800–850 LH2, the B850 Qy transition dipole moments are almost in line and nearly tangential to the circle they form. The B850 pigments form into a ring of nine dimers of 18 Bchl *a* molecules in *Rps. acidophila* and eight dimers of 16 Bchl *a* molecules in *Rs. molischianum*, whereas B800 pigments form a ring of 9- or 8-well separated molecules, respectively. The coupling energy between closely interacting (~9 Å) B850 Qy moments is strong (~250 cm^{-1}), whereas for B800 pigments with relatively large intermolecular distances (>17 Å), the coupling energy is weak (~20 cm^{-1}) (Koolhaas et al., 1998; Krueger et al., 1998). In *Rps. acidophila* and *Rs. molischianum* LH2 complexes, the greatest structural differences are seen between the B800 pigments. In the former, the Bchl *a* macrocycle is within the membrane plane, whereas in the latter it is tilted out of the membrane plane and the Qy transition dipoles are rotated by 90° relative to the nearest B850 neighbor (Mc-

Submitted November 13, 2000, and accepted for publication October 26, 2001.

Address reprint requests to Dr. Miroslav Z. Papiz, CLRC Dresbury Laboratory, Keckwick Lane, Warrington, Cheshire WA4 4AD, United Kingdom. Tel.: 01925-603388; Fax: 01926-603124; E-mail: m.papiz@dl.ac.uk.

0006-3495/02/02/963/15 $2.00

Dermott et al., 1995; Koepke et al., 1996; Freer et al., 1996). In addition, the B800 ligand within LH2 of *Rps. acidophila* is an *N*-terminal formyl group (α-fMet1), whereas in *Rs. molischianum* it is α-Asp6.

All B800–850 complexes seem to be functionally similar as far as their spectral properties and energy transfer dynamics are concerned. The two structures determined so far are examples of LH2 complexes that are expressed as a single type under all light conditions, although they are expressed most plentifully under high-light (HL) (Gardiner et al., 1993).

At low-light (LL) two different LH2 complexes have been observed. The first type is spectrally shifted from B850 to B820; examples of these LL B800–820 complexes are found in *Rps. acidophila* strain 7750 and *Rps. cryptolactis* (Sturgis et al., 1995). The spectral shift has been ascribed to the loss of H-bonds with the B850 acetyl groups (Fowler et al., 1992, 1994). Apart from the spectral blue-shift, B800–820 LH2 complexes seem to be similar to B800–850 complexes (McLuskey et al., 1999). The second type of LL LH2 is a B800–850 complex with a much reduced absorption at 850 nm. This type of complex is found in *Rps. palustris* where A_{800}/A_{850} absorption ratios of 2:1 and 3:1 have been reported in the literature (Evans et al., 1990; van Mourik et al., 1992). It has been suggested, from resonance Raman measurements, that a weakening of the 850 nm peak may be attributable to heterogeneity in the peptide composition, and that the LL complex may be composed of a mixture of B800–850 and B800–820 peptides (Gall and Robert, 1999). As H-bond loss is usually associated with a spectral shift to B820, a reduced absorbance at 850 nm without the appearance of absorption at 820 nm seems to be an anomaly. LL LH2 from *Rps. palustris* exhibits an intricate absorption structure and a strong circular dichroism (CD) signal in the 800 nm region (van Mourik et al., 1992), indicating that there may be at least three different Bchl *a* environments or exciton-coupled energy states. Other essential differences are a 20% increase in the Bchl *a*/peptide ratio (Evans, 1989; van Mourik et al., 1992) and a heterogeneous peptide composition (Evans et al., 1990; Tadros et al., 1993). The proposed heterogeneity arises from the expression of up to five $\alpha\beta$ peptide pairs (Tadros et al., 1993) and the inability to prepare a pure B800–820 despite evidence for the breakage of H-bonds (Gall and Robert, 1999). Recently, we have shown that LL LH2 complexes can be prepared from *Rps. palustris* with progressively increasing A_{800}/A_{850} ratios that is strongly correlated with the emergence of one dominant $\alpha\beta$ peptide pair (Tharia et al., 1999). The complete absence of absorption at 850 nm suggests that previous studies involving LL LH2 contained significant amounts of B800–850 complex.

In this work we present the low-resolution electron density and NIR spectra of a LL B800 LH2 complex from *Rps. palustris*. The absence of absorption at 850 nm highlights the unique nature of this complex and presents several interesting questions concerning the role of B800 pigments in photosynthesis. In B800–850 complexes, the B800 pigments capture and transfer energy within 1 ps to the B850 pigments, to LH1 in ~5 ps, and finally to the reaction center (RC) in ~35 ps (Monshouwer et al., 1995; Zhang et al., 1992; Freiberg et al., 1996; Hess et al., 1995; Nagarajan and Parson, 1997; Visscher et al., 1989). The B800 pigments are involved in energy trapping and intracomplex energy transfer, whereas the B850 pigments also transfer energy between complexes. The absence of an 850 nm band in LL B800 raises two questions: how is intercomplex energy transfer achieved and what is the fundamental nature of this LL adaptation that leads to a concentration of absorption at 800 nm? The answers rely on an adequate description of the excited state energy structure, which in turn is determined by the three-dimensional arrangement of pigments in the complex. We compare observed and calculated NIR absorption and CD spectra of the B800 LH2 complex based on a number of pigment geometries and show that the models which best fit the spectroscopic data are also consistent with the electron density at 7.5 Å resolution. Finally we speculate on the properties of this novel B800 complex and the role it plays in photosynthesis.

MATERIALS AND METHODS

Bacteria and culture conditions

Rps. palustris strain 2.1.6 was grown anaerobically in the light at 22°C in a purpose-built thermostated enclosure fitted with a dimmer switch and monitored with a digital light-meter. HL grown cells with an A_{800}/A_{850} absorption ratio of 1.0 were transferred into growth media containing succinate as the carbon source and illumination at the cell surface was 90 lx. Growth curves were determined by monitoring the absorbance of the culture at 650 nm. Cells were harvested when the A_{800}/A_{850} ratio measured between 1.70 and 1.77.

Purification and spectral measurements

LL LH2 was purified from membranes after the passage of whole cells through an ice-cold French pressure cell (SLM Aminco Instruments, Urbana, IL). Membranes were collected by centrifugation, resuspended in 20 mM Tris-Cl pH 8.0, adjusted to an optical density $(OD)_{800nm}$ of 30 cm^{-1} and solubilized by the addition of 1.0% laurylmaltoside at room temperature (RT) for 8–12 h. Unsolubilized material was removed by centrifugation at 12,000 rpm for 20 min. LH2 was separated from the bulk of the RCs on stepped sucrose density gradients (0.2–0.8 M) containing 0.1% laurylmaltoside. Further purification of B800 complex from the bulk of the LH2 was achieved using a mono-Q ion-exchange column eluted with an NaCl gradient in 20 mM Tris-Cl pH 8.0 containing 0.1% laurylmaltoside. B800 complex eluted at 60–70 mM NaCl; fractions were collected and assayed spectrophotometrically (250–900 nm). The ratio of A_{800}/A_{850} was used as a reference for determining sample purity. CD spectra were measured between 450–1000 nm at RT and at 99 K at the Biotechnology and Biological Sciences Research Council CD Facility, Glasgow University.

Bchl *a* and protein determination

Bchl *a* measurements were made by extraction from a small volume of LH2 in an excess of ice-cold acetone:methanol (7:2) agitated in the dark for

1.5 h at 4°C. The Bchl *a* concentration of the resulting supernatant was determined using an extinction coefficient of 76 mM^{-1} cm^{-1} (Clayton, 1963). Protein content was estimated at 595 nm using Coomassie (Pierce Chemical, Rockford, IL) plus reagent with bovine serum albumin as a standard protein.

High-performance liquid chromatography (HPLC) analysis

LH2 samples were prepared as before (Tharia et al., 1999). Samples were freeze-dried and extracted in chloroform:methanol (1:1) containing 0.1 M ammonium acetate. The peptides were separated from the bulk of the pigments by passage through an LH60 gel filtration column equipped with an ultraviolet detector. Pooled fractions were concentrated by rotary evaporation and were injected onto an HPLC C8 reversed-phase column (Hewlett Packard 1100 series, Palo Alto, CA). The α and β peptides were separated using a 30–100% acetonitrile gradient for over 60 min. Peak fractions were collected and dried under vacuum in preparation for microsequence analysis.

Crystallization conditions and data collection

Crystals were grown by vapor diffusion in sitting drops. LH2 protein containing 0.1% laurylmaltoside and 3.0% (w/v) heptanetriol was used at an OD_{800nm} of 100 cm^{-1}. Protein was mixed in a 1:1 ratio with a reservoir buffer containing 20% (v/v) polyethylene glycol 600, 50 mM Ca^{2+}, and 20 mM Tris-Cl, pH 8.0. Crystals grew within 4 weeks at 15°C. A 7.5-Å dataset was collected at RT from a single crystal on Station 9.6 of the CLRC Synchrotron Radiation Source, Daresbury, UK. Diffraction was observed in one direction to 5.5-Å resolution but only to 7.5 Å in the others. Forty-five images were collected (1.0° rotation, 60 s exposure time) with the ADSC Quantum 4 charge-coupled device detector at a wavelength of 0.87 Å. Data were processed with MOSFLM (Leslie, 1990). The cell dimensions were $a = b = 133.8$ Å and $c = 163.4$ Å, and the systematic absences agreed with the assignment for the space group of $P4_22$. The R_{merge} based on intensities was 0.064 with 99.4% completeness and a multiplicity of 5.6.

Structure Determination

Self-rotation functions were calculated at 7.5 Å resolution with the program MOLREP (Vagin and Teplyakov, 1997). In polar space (*a*/*b* plane defined as $\omega = \pi$, $\phi = 0, 2\pi$), a search for NCS 8- and 9-fold symmetry at $\chi = 45°$ and $\chi = 40°$ revealed a strong peak at $\omega = 90°$, $\phi = 45°$. The peak was broad, however, spanned a wide range of χ values, and was unable to establish the symmetry of the oligomer. At $\chi = 180°$ a continuous band of peaks was found running over all ω values at $\phi = 45°$ and $-45°$. For LH2 data of *Rps. acidophila* and *Rs. molischianum*, these self-rotation peaks are associated with pseudodiads normal to the oligomeric axis relating one repeating unit with the next. With low-resolution data it is not possible to resolve the numbers of peaks and establish the symmetry of the complex unambiguously. However, the peak positions are suggestive of an oligomeric axis in the *ab* plane on or parallel with the *ab* diagonal. For this space group, a crystallographic *ab* diagonal diad exists at $z = 1/4$ and $z = 3/4$, and the possibility that the molecular symmetry is incorporated into crystallographic symmetry has to be considered. This kind of superimposition of symmetries has been observed in previous LH2 structures. To confirm the oligomeric nature of the complex and its position in the cell, two search models were used; the nonameric LH2 structure of *Rps. acidophila* and an octameric model created from a single repeating unit. The program EPMR (Kissinger et al., 1999) was used for the cross-rotation search without packing function constraints to allow for a superimposition of structures if only 50% of the complex formed the asymmetric unit (i.e., if the structure was on the crystallographic diad). For the nonamer there was an additional constraint that it should not be on a diad axis. The nonamer model gave solutions that were statistically worse and with overlapped packing in the cell. The octamer model gave the best solution with a correlation coefficient (CC) of 0.46, placing the complex center to within 2.5 Å of $z = 1/4$ and with the 8-fold axis 2° from being parallel to the diad axis. A similar solution was found using the octameric structure from *Rs. molischianum*, but the statistics for this model were slightly worse than for the synthesized model, and it was discarded at this stage. For the best model, the electron density was refined by noncrystallographic symmetry averaging of four repeating units, solvent flattening, and histogram matching using the program DM (Cowtan and Main, 1993). A protein mask was calculated from one NCS unit and phase extension with noncrystallographic symmetry matrix refinement was performed from 12.0 to 7.5 Å. During this procedure the protein mask was re-calculated twice. The initial protein mask was calculated from a model containing the shorter *Rps. acidophila* peptides and did not accommodate the longer *d* peptides of *Rps. palustris.* However, as the protein mask was refined and extended, new density was naturally incorporated into the structure. During this procedure the mean figure of merit changed from 0.14 to 0.83 and the mean NCS electron density CC changed from 0.56 to 0.91 with an *R* factor of 0.26 between observed and DM-refined amplitudes. The average change in protein phase from that of the starting model was 67°, indicating a significant change in electron density. The CCP4 program suite (1994) was used in most of the structural calculations. Atomic models and electron density was viewed with the molecular graphics program O (Jones et al., 1991). Persistence of Vision Ray tracer (POV-RAY 3.1g; http://www.povray.org) was used to render molecular structures and electron density.

Simulation and fitting spectra

The Hamiltonian matrix elements that describe the excited states are:

$$H_{ij} = E_{ij} + V_{ij};$$

$$E_{ij} = 0 \quad \text{when } i \neq j \quad \text{and} \quad V_{ij} = 0 \quad \text{when } i = j \quad (1)$$

E_{ii} is the site energy of the *i*th pigment and $V_{ij} = \Sigma e_{\alpha i} \cdot e_{\beta j}/r_{\alpha\beta ij}$ is the dipole-dipole interaction energy of the *i*th and *j*th pigments within which the αth and βth atoms have point electric charges $e_{\alpha i}$ and $e_{\beta j}$ separated by the distance $r_{\alpha\beta ij}$. A point monopole approximation (Weiss 1972; Philipson et al., 1971) was used to calculate V_{ij} with the monopole charge divided into half charges placed 1.0 Å above and below the atom and the plane defined by the atom and its nearest neighbors. Inhomogeneous energy broadening was introduced by applying a Gaussian distribution of $\sigma = 170$ cm^{-1} (Jimenez et al., 1997; Monshouwer et al., 1997) to the pigment site energies E_{ii}. For the simulation, 5000 spectra were calculated each with a different set of perturbed energies. The solution of each Hamiltonian gives *k* exciton energy eigenvalues (E_k) and eigenvector coefficients (C_{lk}), *l* denotes the index of each pigment excited state wave function. The dipole (D_k) and rotational (R_k) strengths can then be calculated:

$$D_k(\nu_k) = \sum_{i,j} \mu_i \cdot \mu_j \, C_{ik} C_{jk} \quad (2)$$

$$R_k(\nu_k) = \sum_{i,j} \nu_k \, \mu_j \cdot S_i \times \mu_i \, C_{ik} C_{jk} \quad (3)$$

where ν_k is the absorbing frequency of the *k*th exciton level, μ_i is the *i*th pigment Qy transition dipole moment vector, and S_i is the pigment position vector from a common origin. Individual pigment Qy transition dipole magnitudes, calculated by the monopole method, were rescaled to observed values (Weiss, 1972) and corrected for the dielectric constant of 1.5. Thermal and homogeneous broadening was applied to reproduce spectra at 290 K (Cupane et al., 1995). As for B800–850 from *Rps. acidophila* (Alden et al., 1997), three vibronic modes (20, 200, 700 cm^{-1}) and homogeneous broadening of 150 cm^{-1} were used for the states dominated

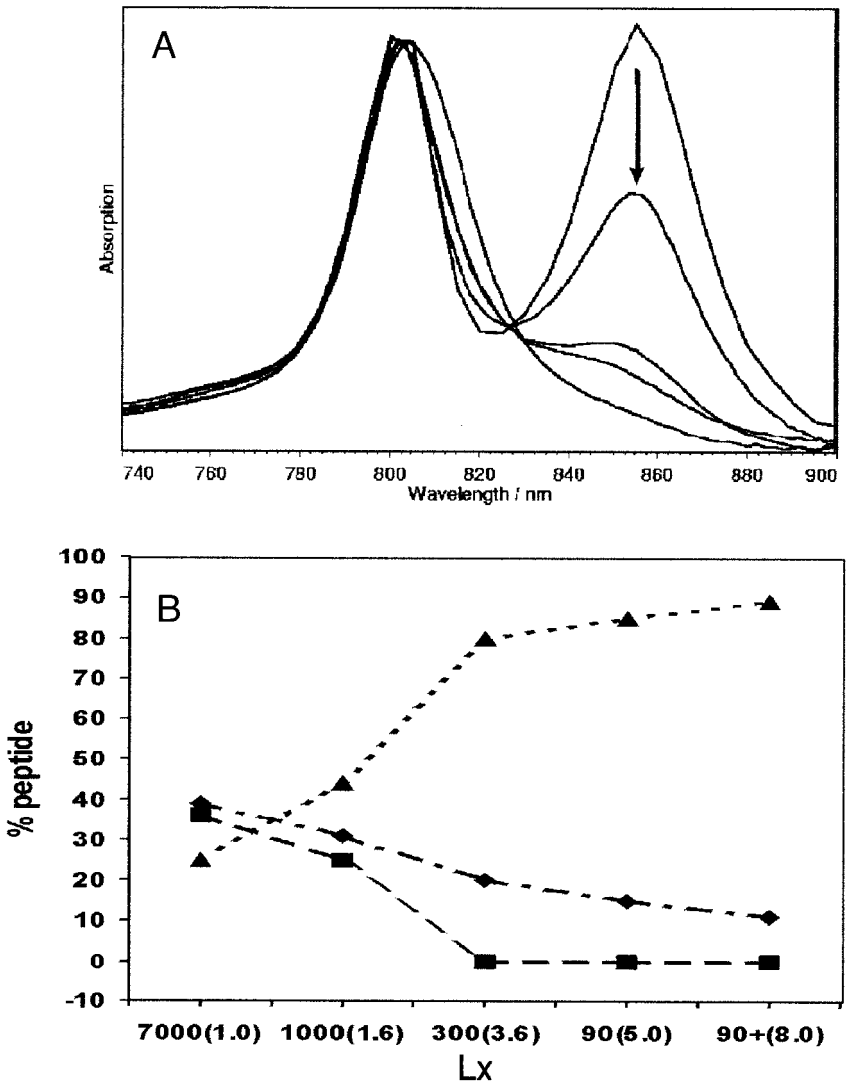

FIGURE 1 (*A*) Absorption spectra of LH2 from *Rps. palustris* grown under different light illumination flux per area (7000, 1000, 300, 90 lx). Spectra were scaled to equal intensities at 800 nm. The arrow indicates decreasing light intensity with absorption ratios A_{800}/A_{850} of 1.0, 1.6, 3.8, 5.0, and 8.0. The 8.0 ratio sample was prepared with an additional mono-Q ion-exchange column purification step. (*B*) Percentages of $\alpha\beta$ *a* (◆), *b* (■), and *d* (▲) peptides isolated by RP-HPLC from cells grown at 7000, 1000, 300, and 90 lx. In parentheses are the A_{800}/A_{850} ratios for each light intensity. Percentages are calculated from the sum of the α and β HPLC peaks for a single peptide type.

by B850 pigments and 2.0 cm^{-1} for B800 pigments and for the $k = 0$ exciton level. Details of vibronic modes and homogeneous broadening have not been established for LL B800 LH2, but at higher temperatures inhomogeneous broadening and Boltzmann thermal effects dominate the spectra. The best fit to the data required a randomly distributed inhomogeneous disorder of $\sigma = 170$ cm^{-1}. The goodness of fit between observed and calculated spectra was monitored by calculating the CCs for their absorption and CD spectra.

RESULTS

LL LH2 peptide composition

LH2 complexes of *Rps. palustris* were purified from cells grown under different light intensities with A_{800}/A_{850} ratios between 1.0 and 5.0. The peptides were isolated by reverse-phase HPLC and identified by sequence analysis (Tharia et al., 1999). Further purification has resulted in LL LH2 complexes with ratios between 8:1 and 20:1. The data show a close and unambiguous correlation between the increase in absorption ratio and the presence of $\alpha\beta_d$ peptides in the sample (Fig. 1, *a* and *b*). It is possible to extrapolate for samples with higher ratios and predict that the best samples of LL B800 complex contain >95% $\alpha\beta_d$ peptides. At 7000 and 1000 lx, three types of LH2 complexes were observed; two composed of $\alpha\beta_a$ and $\alpha\beta_b$ peptides and identified by sequence homology to be B800–850 complexes and one B800 complex composed of $\alpha\beta_d$ peptides. Below 300 lx, the B800–850 $\alpha\beta_b$ complex is absent as judged by HPLC analysis (Tharia et al., 1999). The B800–850 complexes

can be identified as such because they contain α-Tyr(+13)-Trp(+14) (relative to the His(0) ligand of B850), which are capable of H-bonding to the Bchl *a* C3-acetyl groups whereas the α_d peptide has Phe(+13)-Met(+14) at these positions and would therefore be expected to exhibit a B800–820-like spectrum.

Bchl *a* content

The Bchl *a*/peptide ratio of LL B800 LH2 with an A_{800}/A_{850} ratio of 8:1 was determined to be 4.2 ± 0.3. The Bchl *a*/peptide ratio for B800–850 LH2 of *Rps. acidophila*, determined at the same time, was 3.2 ± 0.3. In calculating the ratio for B800 LH2 samples, an average combined α/β peptide molecular weight of 11,959 au was used, as the sample was estimated to contain ~10% $\alpha\beta_a$ peptides (Fig. 1 *b*). Our calculations suggest four Bchl *a* molecules per repeating unit in LL B800, and not three as determined for B800–850 complexes. A Bchl *a*/peptide ratio of 4.5 has been reported for the B830 LH2 complex of *Chromatium purpuratum* (Kerfeld et al., 1994), a purple sulfur bacterium which is believed to be evolutionarily more ancient than the purple nonsulfur bacteria. B830 LH2 from *Chr. purpuratum* has similarities with LL B800 of *Rps. palustris* in that it has one predominant peak at 830 nm with a small shoulder at 802 nm. Although the peptides in this B830 complex do not vary in response to changes in light intensity, a heterogeneous expression of 3 $\alpha\beta$ peptide pairs is observed.

NIR spectra

LL B800 LH2 has very different absorption and CD spectra compared with B800–850 LH2 of *Rps. acidophila*. The absorption spectrum is a single peak, centered at 802 nm, and is slightly broadened on the red side with a full-width-half-maximal height of 400 cm^{-1} comprising 190 cm^{-1} in the blue and 210 cm^{-1} in the red (Fig. 2 *a*). The full width half-maximal value is similar to LH2 from *Rps. acidophila*, which has 405 cm^{-1} and 345 cm^{-1} for the 850 nm and 800 nm peaks, respectively. The LL CD spectrum has a large positive band at 813 nm and two smaller negative bands at 800 and 832 nm (Fig. 2 *b*). An important feature is the nonconservative nature of the peaks at 813 and 831 nm (i.e., peaks of opposite sign are not of equal intensity), whereas for B800–850 LH2 a conservative pair of peaks are observed in this region.

The 99 K CD spectra of B800 and B800–850 complexes from *Rps. palustris* and B800–850 LH2 from *Rps. acidophila* show important differences compared with RT spectra (Fig. 2 *c*). At 800 nm the B800–850 spectra are almost identical for both species at 99 K. Their positive and negative bands are closer to the zero crossover point by ~5 nm relative to the RT spectra, and this change may be attributable to thermal broadening. In the region of 850–890 nm, the peaks are at slightly different energies in the two species but with very similar shapes and at 99 K they are red-shifted by 12–18 nm relative to the RT spectra. In contrast, the red-most negative band of LL B800 shifts to the blue, from 832 to 824 nm. In addition, the relative intensities of the two negative bands are reversed in comparison to the RT spectra, with the 803 nm band more intense. The LL B800 CD spectrum seems very intense, but when compared with B800–850 spectra, the sum of the modulus of rotational strengths for LL B800 is only 30% greater. The origins of the energy shifts for the lowest-energy bands, upon cooling, in B800 and B800–850 LH2 are not known. They may be attributable to specific chemical and structural changes in each of these LH2 complexes. However, a simple explanation of the CD observations may be because of an increase in coupling energies between pigments. This would shift the high-energy branch of the exciton band into the blue and the low-energy branch into the red. The origin of the two branches, in B800–850 complexes, is attributable to progressive energy splitting through pigment-pigment energy coupling between the nearest and then between the more distantly separated pigments. The splitting caused by nearest neighbor interactions is the largest and establishes the upper and lower energy branches centered about the monomer pigment energies. Hence, any increase of coupling energy will push the high-energy branch to even higher energies and the low-energy branch to lower energies. In LL B800, the blue-shift of the 832 nm band to 824 nm could indicate that these exciton energy levels may lie in the high-energy branch. The corollary of this is that the 850 nm bands of B800–850 complexes occupy the lower branch, and, therefore, one would predict a red-shift by this mechanism; this is exactly what we observe.

The complete absence of absorption and CD signal in the 850–880 nm region indicates that the LL B800 complex is a new type of complex and different from the B800–820 and B800–850 complexes. The cause of the single band at 800 nm may be because of local chemical changes that blue-shift pigment (site) energies. In addition there may be a reorganization of pigment geometries that move the strongly absorbing bands into the high-energy branch of the exciton manifold. These questions will be explored in a later section.

Crystal structure packing

The electron density of LL B800 complex from *Rps. palustris* was calculated at 7.5-Å resolution (Fig. 3). The crystal symmetry is $P4_222$ with the 8-fold axis of the B800 complex incorporated into the crystallographic diad axes on the *a*/*b* diagonals at $z = ¼$ and $z = ¾$. Hence, the asymmetric unit comprises just four repeating units. The *C*-terminal surface of one complex is in close contact with another. An unusual feature of the molecular packing is the change in

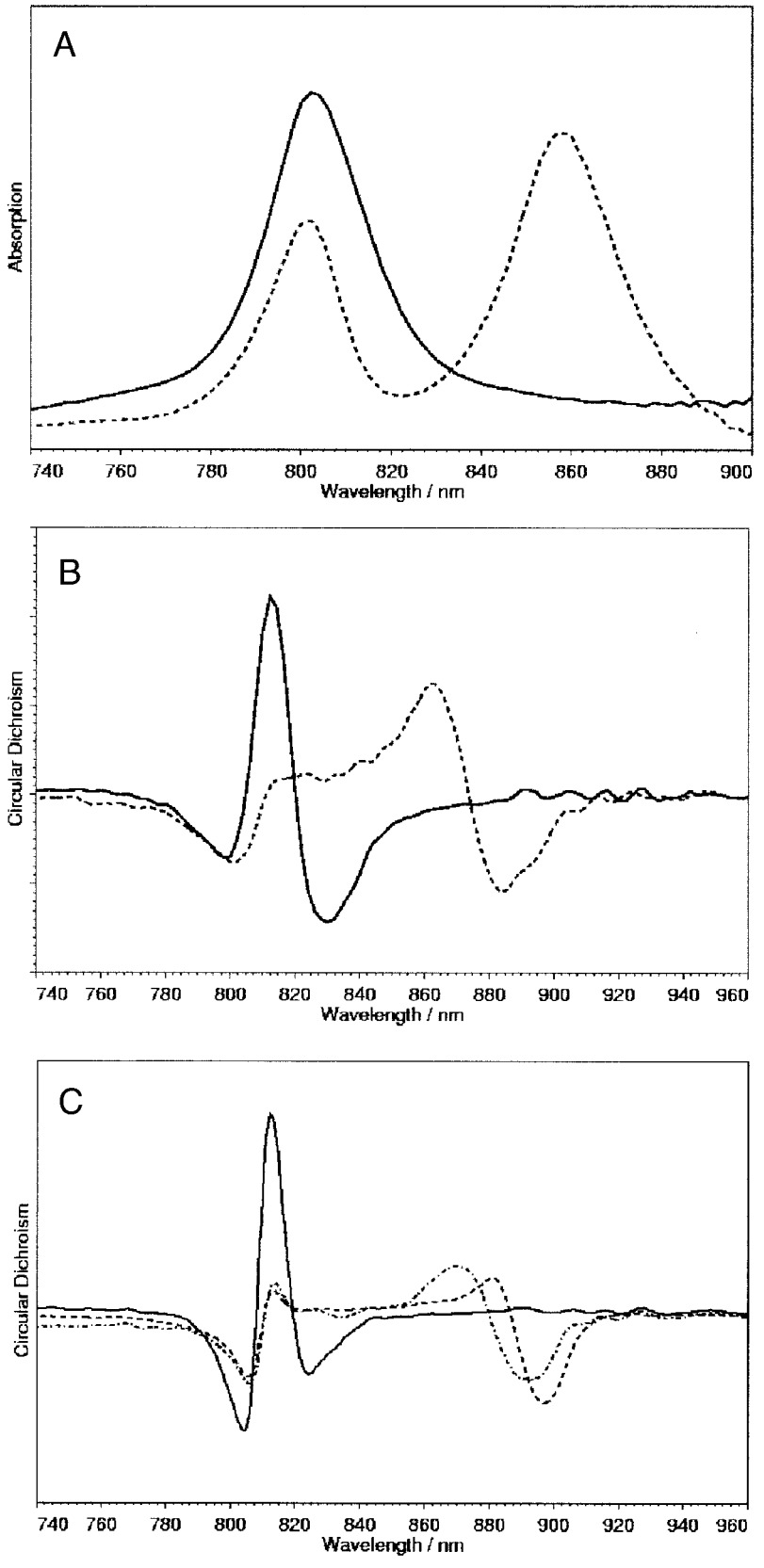
A
Absorption
740 760 780 800 820 840 860 880 900
Wavelength / nm
B
Circular Dichroism
740 760 780 800 820 840 860 880 900 920 940 960
Wavelength / nm
C
Circular Dichroism
740 760 780 800 820 840 860 880 900 920 940 960
Wavelength / nm

FIGURE 3 A slab of electron density from LL B800 LH2 of *Rps. palustris* at 7.5-Å resolution looking along the crystal diad at $z = ¼$ and contoured at 1.0 σ. The complexes forming the horizontal central layer have their eight-fold axes pointing out of the page while the layers above and below form dimers of LL B800 LH2 with eight-fold axes in the plane of the page. Dotted line outlines one complex in a dimer.

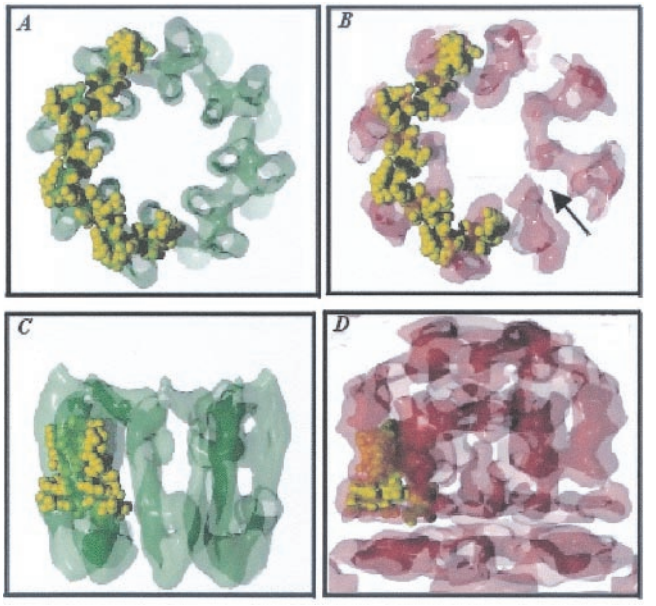

FIGURE 4 Electron densities with a superimposed search model of one asymmetric unit of Bchl *a* pigments viewed into (*A* and *B*) and along (*C* and *D*) the membrane. The green electron density is calculated from the B800–850 derived search model and the red electron density from the LL B800 LH2 x-ray diffraction amplitudes and phases obtained from the molecular averaging and solvent flattening procedure in DM (Cowtan and Main, 1993). The maps (*A* and *B*) at the level of B850 pigments are shown with an atomic model of the B800–850 Bchl *a* molecules superimposed (*yellow*). The arrow in *B* marks the gap between repeating units that is not observed in the model electron density of *A*.

octameric axis direction in alternate layers; the *a*/*b* diagonal at $z = ¼$ followed by another layer at $z = ¾$ and aligned at right angles to the first. This arrangement is different from the packing found for B800–850 LH2 structures of *Rps. acidophila* and *Rs. molischianum*, where the respective 9- and 8-fold axes remain parallel throughout the crystal, forming stacked LH2/detergent layers. The V_m for LL B800 is 5.6, which implies solvent/detergent content of 75%, if we assume a partial specific volume of 0.81 derived from the B800–850 LH2 structures of *Rps. acidophila* (V_m 5.1; 73% solvent) and *Rs. molischianum* (V_m 4.0; 66% solvent).

Electron density

The quality of phases used for the calculation of electron density was greatly improved, over the starting phases, by 4-fold NCS averaging and solvent/detergent (60%) flattening. The absolute phase change was 67°, which indicates that the electron density features within the final electron density map are significantly changed from the starting map. Apart from statistical indicators that are obtained from the electron density modification procedure, which indicate good NCS averaging convergence, the quality of the electron density can also be evaluated in the light of the peptide chain lengths for B800–850 in *Rps. acidophila* and B800 LH2 from *Rps. palustris*. Comparison of the electron density maps derived from the model, which is essentially that of the *Rps. acidophila* B800–850 structure and the NCS-averaged data, reveals important differences. In particular, additional density can be seen at the *N*- and *C*-termini of the B800 LH2 structure that is not found in the model-derived density (Fig. 4 *D*). In the B800–850 LH2 crystal structures (McDermott et al., 1995; Koepke et al., 1996), the peptides are aligned in the same direction with the *C*-termini on one membrane surface and the *N*-termini on the other. Compared with LH2 of *Rps. acidophila*, the *N*-terminus of the β_d peptide in B800 LH2 is longer by 10 residues and the *C*-terminus of the α_d peptide is longer by 6 residues. The *N*-terminus is the "membrane" surface nearest to the B800 pigments in our starting model. This is consistent with the observation that additional density is found emanating from the outer peptides at the *N*-terminus, whereas at the *C*-

FIGURE 2 Measured NIR (*A*) absorption; (*B*) CD spectra at 293 K, and (*C*) CD spectra at 99 K. LL B800 LH2 from *Rps. palustris* with an A_{800}/A_{850} absorption ratio of >10:1 (*solid line*); B800–850 LH2 from *Rps. acidophila* strain 10050 (*dashed line*) and B800–850 LH2 from *Rps. palustris* (*dotted line*). The CD spectra in (*C*) are normalized by the sum of their peak height absorption to approximate the same relative scale of pigment concentration. The sum modular rotational strengths of spectra in (*C*) are 0.22, 0.25, and 0.31 for *Rps. acidophila* B800–850, *Rps. palustris* B800–850 and *Rps. palustris* LL B800, respectively.

terminus, the electron density extends by 10 Å in a direction approximately normal to the membrane, with most of the electron density near the center of the complex forming a cone. This is very reminiscent of the *C*-terminus in B800–850 LH2 of *Rs. molischianum* where the α peptides are also longer and extend from the membrane surface in a similar way (Koepke et al., 1996). These observations are consistent with the longer peptides of *Rps. palustris* and the assignments of the *N*- and *C*-termini based on the starting model alignment. The electron density of the transmembrane α helices is continuous over the main part of this region but is broken near the *N*-termini where the transmembrane helices change to surface helices. Strong electron density can be seen at the positions of the B850 and B800 Bchl *a* molecules. The B850 electron density, calculated from the B800–850 model (Fig. 4 *A*), shows strong features connecting the pigments in a ring, whereas the same electron density obtained from the experimental data shows the LL B800 structure to have less electron density between repeating units, with significant gaps at the position of the B850 Bchl *a* molecules (Fig. 4 *B*; *arrow*). At this resolution we must be cautious in our interpretations, but this does suggest a model comprising a ring of Bchl *a* molecules that are oriented radially, like the spokes of a wheel, rather than tangentially. In the region of the B800 pigments radial protrusions extend outward beyond the model (Fig.4 *D* and 9*C*). The density closest to the *N*-terminus corresponds to the B800 pigments in our search model, whereas the electron density above this is new and unaccounted for, and lies approximately midway between the B850 and B800 pigments. This density does not have a structural counterpart in our molecular replacement model and may belong to the additional pigment that we have identified by extraction methods.

Pigment modeling and calculated absorption and CD spectra

NIR absorption and CD spectra give complementary information on the organization and energies of Bchl *a* pigments. The NIR spectra of LH2 complexes are dominated by Bchl *a* Qy transition dipole moments and present a tractable computational problem for simulation. Several models were considered based on two starting models: (model 1) the B800–850 LH2 structure from *Rs. molischianum* and (model 2) the B800–850 LH2 structure from *Rps. acidophila* modified to an octamer. The *Rps. acidophila*-derived octamer was created from one repeating unit by radial contraction by the factor 8/9, before rotationally copying the unit eight times. The inter-B850 pigment distances were adjusted to keep a uniform separation of ~9 Å. To understand the calculations described below, it is important to note that, although it is commonly stated in the literature that the B850 pigments are tangentially arranged, in fact, the angle that Qy dipole moments make with the radial vector, defined by the circle passing through the Mg atoms, is 106° (α-B850) and 61° (β-B850).

Models with Bchl *a* energy changes alone

The absorption shift from 850 nm to 800 nm can be achieved by an increase in monomeric Bchl *a* energies. Previous simulation of B800–850 LH2 absorption and CD spectra have required Bchl *a* wavelengths between 810 and 840 nm for B850 pigments and 800 nm for B800 pigments (Koolhaas et al., 1997; Alden et al., 1997). In these simulations the Bchl *a* pigments bound to β peptides were found to have lower energies than those bound to the α peptides by ~10–20 nm. The 850 nm region of *Rps. acidophila* and *Rs. molischianum* B800–850 complexes is dominated by the $k = -1$ and $+1$ exciton energy states, whereas the $k = 9$ states in *Rps. acidophila* and $k = 8$ states in *Rs. molischianum* have weak optical strengths and are hidden by the B800 absorption peak. However, the high-energy extreme of the B850 exciton band has been determined to be at ~780 nm from studies on a B800-free B800–850 mutant (Koolhaas et al., 1998). A shift of $k = \pm 1$ energy states to an absorption wavelength of 800 nm requires monomer wavelengths of between 770 and 795 nm for the two models; however, the spectra are poorly fitted (Fig. 5, *a* and *b*), with only two peaks visible in the CD spectrum rather than three. The B850 pigment orientations are almost identical in the *Rps. acidophila* and *Rs. molischianum* models, so the origin of the very different calculated CD spectra must lie in the different B800 orientations in models 1 and 2 and the regularization of the inter-B850 distances at 9 Å for model 2. The red-shifted zero crossing point of the CD spectrum for B800–850 has been explained by the need to involve more than half of the B850 pigments in the calculations, with the consequence that the absorption spectrum shifts to $k = \pm 1$ energy levels as the CD spectrum is equally shared between $k = 0$ and $k = \pm 1$ (Koolhaas et al., 1997). In part, it is this blue-shift of the absorption spectrum relative to the CD spectrum that is incompatible in fitting both the absorption and CD spectra of the B800 complex by monomer energy shifts alone. This can be seen in the better fits of CD spectra when lower monomer energies are assumed; however, this causes the absorption spectra to be badly fitted.

Models with changed B850 orientations

For LL B800 LH2, the Bchl *a* Qy transition dipole moments have been determined by anisotropy and polarization measurements to lie approximately in the membrane plane (van Mourik et al., 1992; Ma, 1998). This agrees with observations for other LH2 as well as LH1 complexes. If the Qy vector can be assumed to lie close to the membrane plane, then this reduces the range of orientations that need to be explored. With this in mind, a shift of absorption from 850

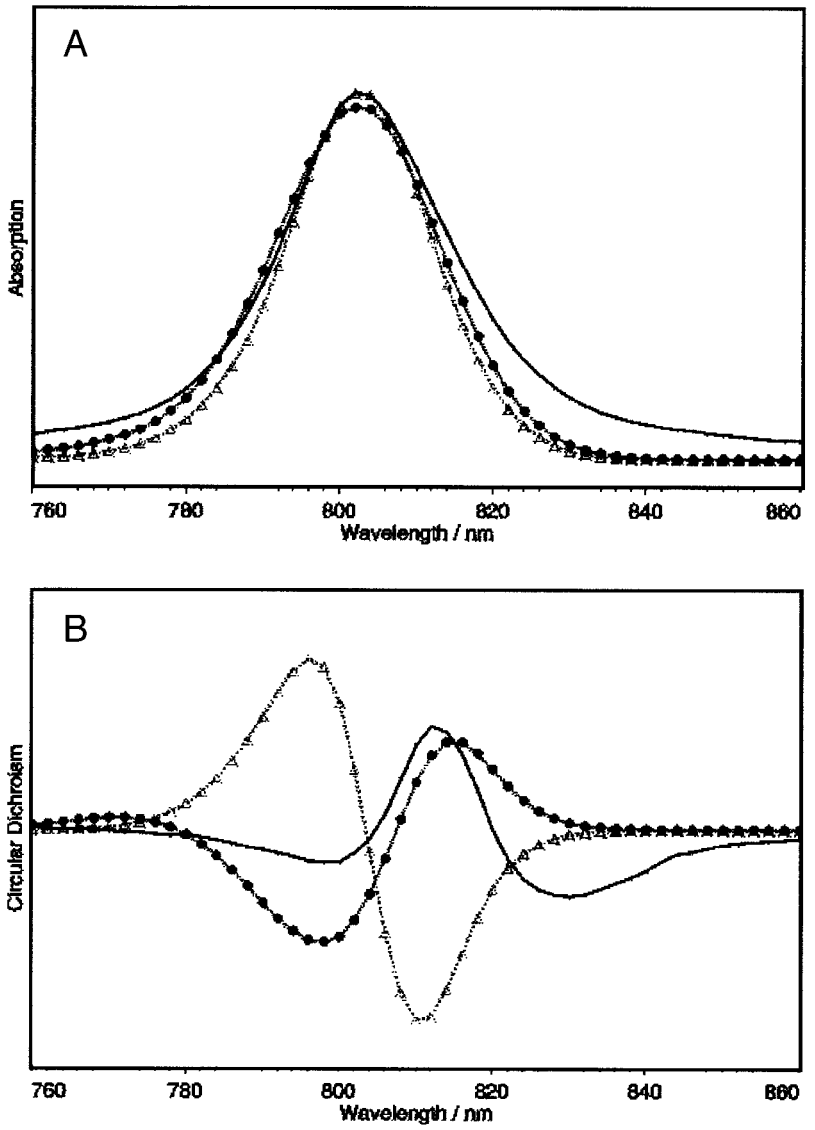

FIGURE 5 Model calculations of (*A*) absorption and (*B*) CD spectra from the B800–850 LH2 structure from *Rs. molischianum* (● model 1) and an octamer derived from the B800–850 LH2 from *Rps. acidophila* (△ model 2). The observed spectra are in solid lines. The B850 monomer energies were varied to reproduce the absorption spectra. For Bchl *a* bound to α and β peptides, these were 770 nm and 770 nm for model 1 and 795 nm and 780 nm for model 2. B800 pigments were given energies of 800 nm.

to 800 nm can be brought about by changing the orientation of the B850 pigment to an approximate radial alignment. This can be achieved by a rotation ϕ about a vector normal to the membrane and passing through the Mg atom of Bchl *a* (Fig. 6 *a*). This causes the higher exciton energy levels to have larger dipole strengths at the expense of the low-lying energy states. At intermediate orientations, dipole strength is shared at the two ends of the exciton band and a bimodal peak distribution is apparent. In such a situation, two absorption peaks would be visible, not one (Fig. 7, *a* and *c*). As already stated, the alignment of the B850 Qy transition dipoles in B800–850 LH2 is 106° and 61° relative to the radial vector, which is defined as a vector in the membrane plane and passing through the center of the complex. A rotation of B850 through an angle of 40° about the membrane normal brings the Qy alignments to 146° and 21° relative to the radial vector. This is sufficient to place the majority of the dipole strength into the blue end of the exciton band producing a unimodal absorption peak distribution.

It is useful at this point to make a distinction between B850 pigments in the B800–850 complex and those in the LL B800 LH2 which we will call B-α or B-β depending on with which peptide they ligand. An undesirable aspect of radial alignment of B-α/B-β pigments is an almost face-to-face arrangement which creates problems for their histidine

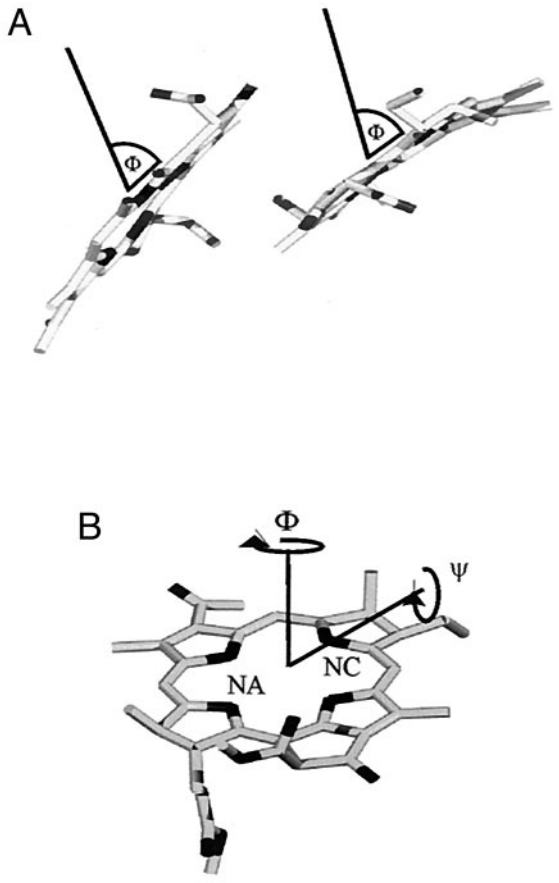

FIGURE 6 Bchl *a* geometries were explored by rotating B-α/B-β pigments about the membrane normal through an angle Φ. B800–1 and B800–2 orientation was explored by a rotation about the membrane normal Φ and by tilting the Qy transition dipole moment out of the membrane plane by an angle Ψ which is defined by the axis of rotation joining atoms NA and NC. (*A*) A view looking into the membrane onto B-α/B-β pigments. (*B*) A view from slightly above the membrane plane at B800.

ligands which compete for the same space. One possible way to avoid this is to stagger the pigments alternately in a radial fashion by $\sim+1.5$ and -1.5 Å. Molecular modeling indicates that this creates sufficient space for the histidines to approach their respective pigments. The calculated spectra are only slightly improved with this modification, as might be expected from such a small change, but it is important to show how the ligand connections to the pigments can be maintained. As seen in Fig. 7, *c* and *d*, it is model 2 with the B-α/B-β pigments rotated 40° about the membrane normal that comes closest to fitting both the absorption and CD spectra. Model 1 fits the CD spectra poorly even after exploring the rotational space more finely. Again this seems to suggest that the B800 orientations and inter-B-α/B-β separations are more similar to model 2. Interestingly, the pigment monomer energies required for such models are in the range of 815–825 nm with lower energies for the pigment bound to the β peptide. These values are more in accord with those used by others to calculate the spectra of the *Rps. acidophila* B800–850 complex, and are more satisfactory than the large blue-shifts required for models based on energy shifts alone, which are typical of energies for Bchl *a* molecules in organic solvents.

The number of Bchl *a* molecules

Our determination of a Bchl *a*/peptide ratio of 4 for LL B800 LH2 requires us to consider models that can accommodate a fourth pigment molecule. The positioning of the fourth pigment is unclear, but inspection of the B800–850 complex indicates that the most likely place for additional pigments is between the B800, B-α/B-β, and the β peptides. A number of other sites were considered, but did not produce reasonable calculated spectra, and were poor when protein/pigment interactions were taken into account. The B800–1 Bchl *a* pigments were at the same position as those in the B800–850 complex whereas the new pigments named B800–2 were positioned approximately halfway between the B800–1 and B-α/B-β. It was found that placing B800–2 too close to B800–1 or B-α/B-β produced unsatisfactory calculated CD spectra. The orientation of the B800–1/B800–2 Qy dipole moments were also investigated at this stage with ϕ and ψ angles varied according to Fig. 6 *b*. The ψ angle is defined by a rotation about a vector joining the NA and NC Bchl *a* atoms and tilts the Qy vector out of the membrane plane. A systematic search of these angles produced two models that best fitted the observed spectra (Fig. 8, *a* and *b*). Model 4, which contained four Bchl *a* molecules per repeat unit, had both B800 Qy moments tilted by $\psi = 10°$ relative to the membrane plane and toward the B-α/B-β pigments. This resulted in the correct relative strengths and positions for the two negative CD peaks at 800 and 832 nm, and gave significant improvements in the absorption and CD CCs of 0.96 and 0.97, respectively. Rotations of $\phi = 45°$, 25°, and 15° were applied to B-α/B-β, B800–1, and B800–2, respectively. For comparison, model 3 with only B-α/B-β and B800–1 pigments was considered with angles $\phi = 40°$ and 15° and $\psi = 0°$ best fitting the data, with CCs of 0.96 and 0.92 for absorption and CD spectra, respectively (Fig. 8, *a* and *b*). For both models, the B-α/B-β pigments were staggered by ± 1.5 Å to accommodate the histidine ligands, and monomer energies were varied to find the best fit. The discrepancy in fit between these models resides mainly in their CD spectra. The negative peak at 800 nm fits well for model 4, whereas for model 3 it is blue-shifted to 790 nm. It is interesting to note that for both models the direction of rotation for all pigments is the same. It would therefore be possible to apply a rotation to the whole repeating unit, comprising an $\alpha\beta$ peptide pair and Bchl *a* molecules, followed by smaller rotations to the individual pigments. This naturally introduces radial stagger for the B-α/B-β Bchl *a* molecules if a center of rotation midway between B-α/B-β pigments is chosen. For example, a rotation of the whole repeating unit

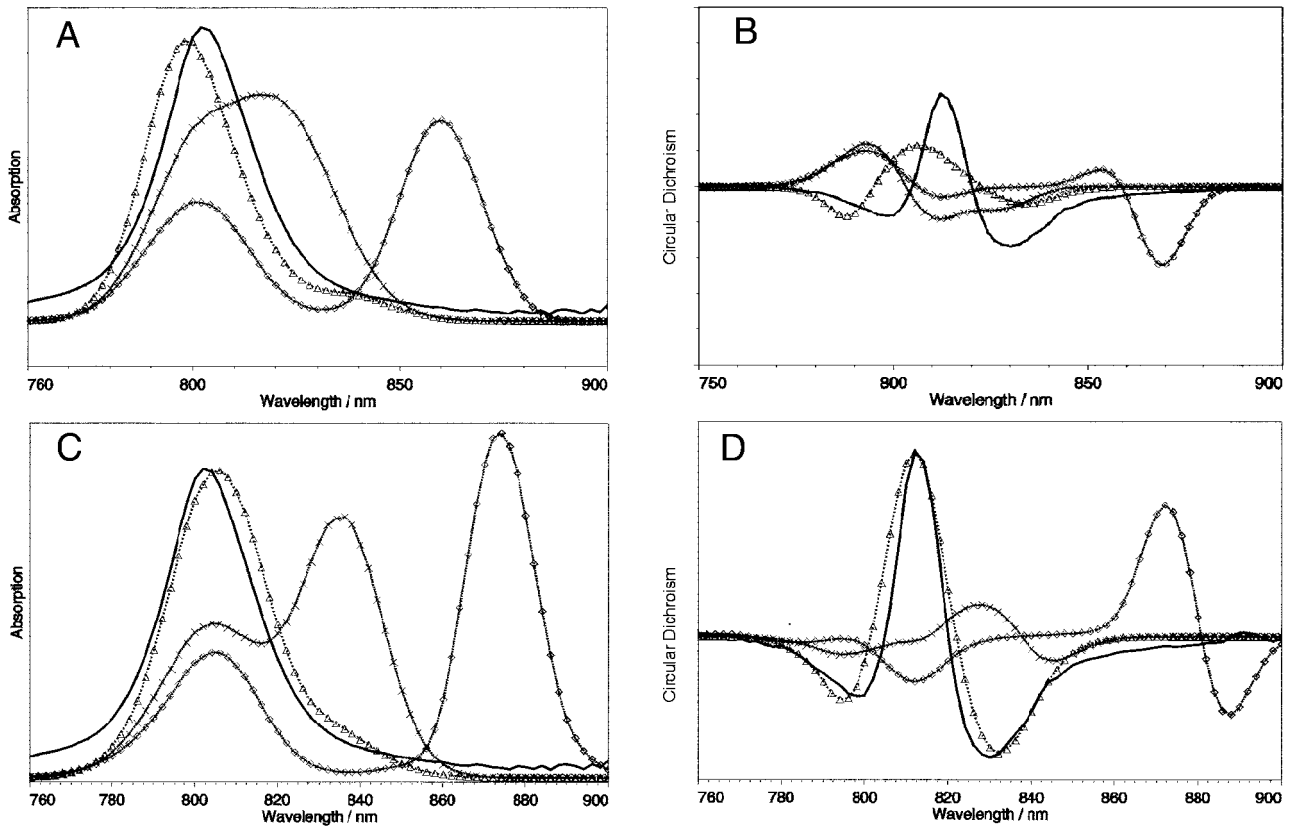

FIGURE 7 The angle of B-α/B-β pigments (Φ) was varied by 0° ($\diamond$), 20° (x), and 40° (Δ) for: *Rps. molischianum* (*A*) and (*B*) and the *Rps. acidophila* derived octamer (*C*) and (*D*). Observed data are solid lines. (*A*) and (*C*) are absorption spectra; (*B*) and (*D*) are CD spectra. The CCs between observed and calculated spectra were: (*A*) 0.51, 0.85, 0.94; (*B*) −0.17, −0.30, 0.59; (*C*) 0.31, 0.61, 0.95; (*D*) −0.20, −0.21, 0.94 at Φ angles 0°, 20°, and 40°, respectively. The monomeric energies of B-α, B-β, and B800 were fixed at 815, 825, and 800 nm, respectively.

by $\phi = 30°$ will stagger the B-α/B-β pigments by ± 1.2 Å, with an additional benefit that there can not be any problems at the histidine ligands as the internal geometry of a repeating unit is unchanged; only the interactions between neighboring units are affected. These independent rotations seem to be additive in their effect so that similar spectral simulations can be obtained by a rotation of the whole unit followed by a smaller rotation of individual pigments.

What seems to be clear from this modeling is that simple monomer energy shifts are not sufficient to account for the absorption and CD spectra, and the most important change to the structure that explains the data requires a rotation of B-α/B-β Qy transition dipole moments so that they lie within 20–30° of the radial vector. Although some improvement is obtained for model 4, the presence or absence of the additional B800–2 pigments seems to be masked by the similarity in the B800 orientations. There is evidence for the presence of an additional Bchl *a* molecule in the 7.5-Å electron density map, which when compared with the starting model electron density shows a strong feature at the expected position (Fig. 9, *b* and *c*). Even at this resolution, it is clearly possible to distinguish features such as Bchl *a* pigments, as seen by the protrusions in both calculated and data-derived maps. However, it really requires a high-resolution x-ray structure to unambiguously assign the density. Apart from the biochemical evidence that we have presented for four Bchl *a* molecules per $\alpha\beta$ pair in the B800 LH2 of *Rps. palustris*, a previous report estimates 20% more Bchl *a* per peptide ($\equiv$ 3.6:1 Bchl *a*:peptide ratio) (Evans, 1989; van Mourik et al., 1992) and an estimated Bchl *a*/carotenoid ratio of 1.98:1 for B800–850 and 3.05:1 for LL LH2 (Evans et al., 1990). These values can be understood if we estimate ~40% B800–850 contamination in the LL LH2 samples used in these experiments. The estimate of contamination is determined from the A_{800}/A_{850} ratios of the samples used and then assigning the peptide composition from our HPLC data (Fig. 1 *b*). If an appropriate correction is made, their results would seem to indicate, almost exactly, four Bchl *a* molecules per repeating $\alpha\beta$ unit and four Bchl *a* molecules per carotenoid.

It is difficult to choose between models 3 and 4, based on modeling alone. However, taken with the evidence of the experimentally determined Bchl *a*/peptide ratio of 4, the features in the low resolution electron density map and the marginally better spectral fit using four pigments rather than three, a model similar to model 4 is strongly favored (Fig.

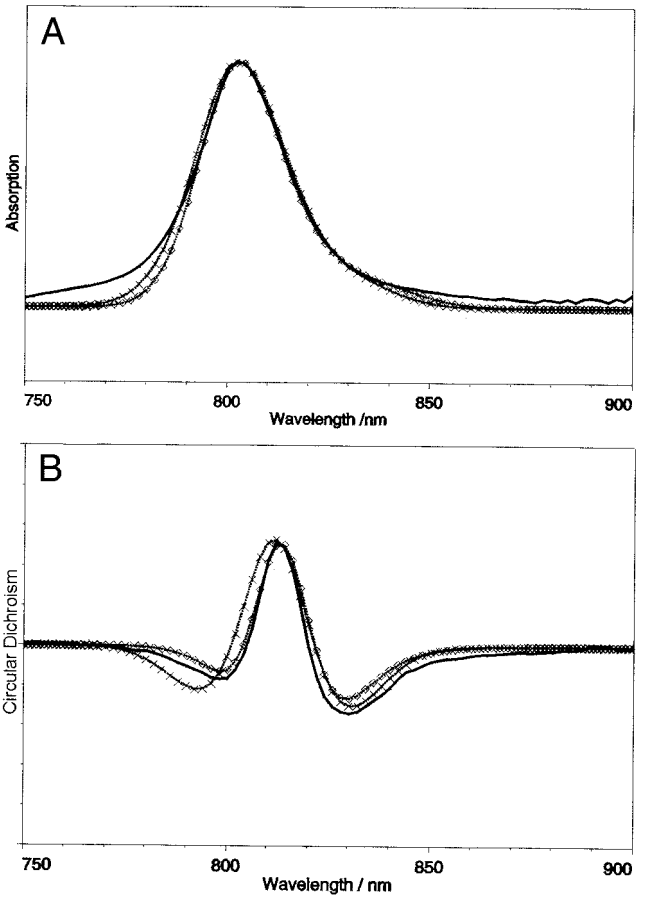

FIGURE 8 (*A*) Absorption and (*B*) CD spectra. The observed spectra are in solid lines. Calculated spectra for model 3 (×) and model 4 (◇). The absorption and CD spectra CCs for model 3 comprising three Bchl *a* molecules per repeat are 0.96 and 0.92, respectively. For model 4, comprising four Bchl *a* molecules per repeat, the CCs are 0.96 and 0.97, respectively. Monomer pigment energies for B-α and B-β of model 3 are 817 nm and 819 nm, and for model 4 are 813 nm and 826 nm. B800 pigment energies in the two models were 800 nm. Homogeneous broadening of 150 cm^{-1} was used for the states dominated by B-α and B-β pigments and 2.0 cm^{-1} for B800 pigments and for the $k = 0$ exciton level. Inhomogeneous disorder with 170 cm^{-1} Gaussian width was used for all pigments.

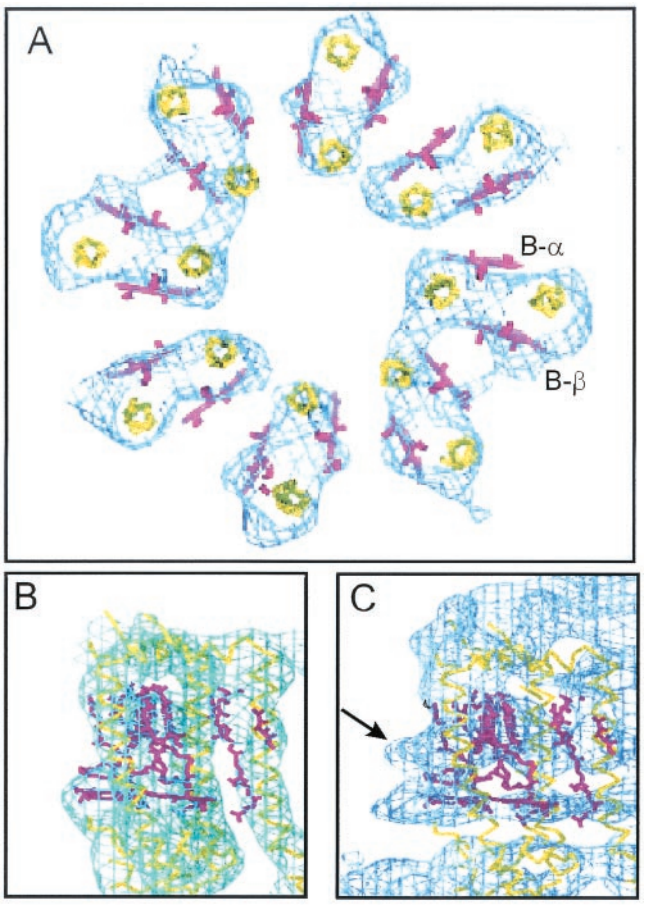

FIGURE 9 The electron densities obtained from LL B800 LH2 x-ray data after NCS averaging and solvent flattening are shown in blue (*A*) and (*C*), and the electron density calculated from the starting B800–850 octamer model is shown in cyan (*B*). Electron density (*A*) is looking down the octameric axis with the B-α and B-β pigments (*magenta*) superimposed in the orientations for models 3 and 4; the helices linking C α atoms are shown in yellow. The view for (*B*) and (*C*) is along the membrane surface, with the starting B800–850 model superimposed. For (*B*) and (*C*) the center of the complex is on the right and the *N*-terminus is at the bottom of the image. The additional electron density above B800 Bchl *a* is indicated with an arrow in (*C*).

10). It must be stressed, however, that the exact location of the fourth pigment is less certain than the other pigments as lateral translation in the membrane plane has less effect on the spectra.

DISCUSSION

It is clear that the B800 LH2 constitutes a unique complex with different spectral properties to B800–850 complexes. Although the details of the exciton structure must await a high resolution structure and further spectroscopy measurements, it is interesting to speculate on the nature of this LL adaptation in *Rps. palustris*.

The pigment density of LL B800 complex is almost a factor of 2 greater than in B800–850 complexes. This estimate is based on the additional pigment per repeating unit and the slightly smaller diameter arising from the octameric rather than nonameric arrangement of units. In addition, solar energy passing through air and the water environments in which these bacteria are found has been measured and shown to fall off at longer wavelengths (Vila et al., 1996). The combined effect of greater pigment density and a shift to a more intense part of the solar spectrum gives the opportunity for increased light trapping and may, in part, explain the reason for this LL adaptation. However, this presents a new problem for energy transfer to the LH1/RC as shifting the absorption maxima from 850 to 800 nm increases the energy gap by ~700 cm^{-1}. The actual gap

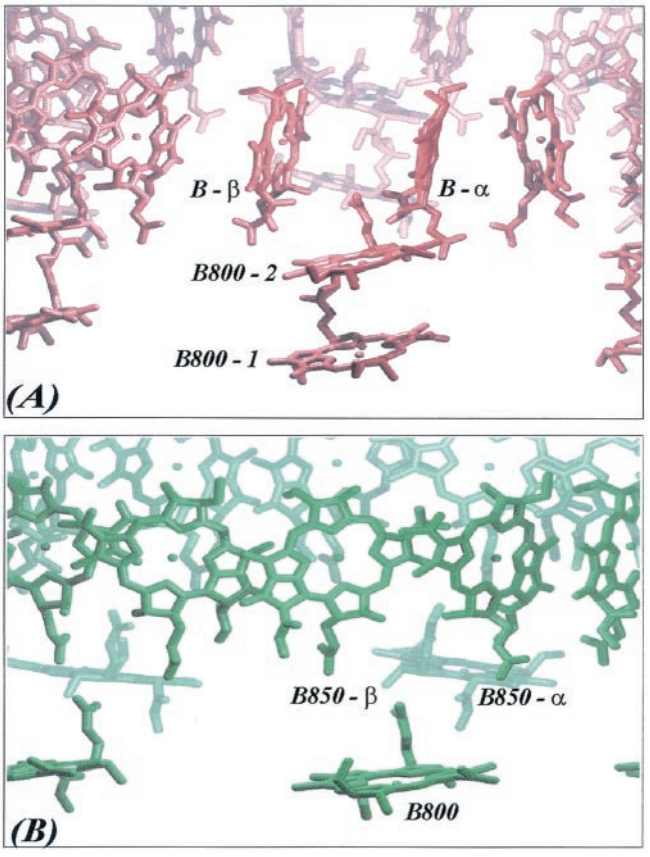

FIGURE 10 (*A*) Bchl *a* molecules of model 4 (*red*) and (*B*) Bchl *a* molecules from the B800–850 LH2 of *Rps. acidophila* (*green*). B-α, B-β, and B800–1 are equivalent to B850-α, B850-β, and B800 in B800–850 LH2, but are re-oriented whereas B800–2 are the additional pigments in model 4. Model 3 (not shown) is as in (*A*) with the B800–2 absent and the plane of B800–1 exactly in the membrane plane. The view is approximately in the plane of the membrane.

may be less, as there is a pronounced tail on the red side of the 800-nm band and there may be weaker excitation states at lower energies involved in energy transfer. However, the interesting questions are: how are the various B800, B800–850, and LH1/RC complexes arranged in the membrane and are there any biological advantages that mitigate the effects of this large energy gap?

Time-resolved emission measurements on *Rps. palustris* membranes (Nishimura et al., 1993) have shown rapid relaxation of energy to B824 pigments and then to B850 within the same complex, with final energy transfer to LH1/RC. This was found to coexist with independent domains of B800–850/LH1/RC. However, this was in a different strain of *Rps. palustris* and it is not clear which LH2 complexes were being expressed. Nevertheless their work indicated the presence of two distinct domain types. The ability to switch from B800–850 to B800 LH2 production may be to improve RC trapping efficiency, as was shown in the LL adapted B800–820 complex (Deinum et al., 1991), where B800–820 maintained an effective barrier against back transfer of energy from LH1/RC. A photosystem containing B800–850/LH1/RC can transfer energy from the LH1/RC core back to LH2 (Freiberg et al., 1996; Timpmann et al., 1995). This may only be a requirement under HL conditions, when significant numbers of RCs are in a photoxidized state and high trapping efficiency can continue to be maintained by a reverse energy flow to RCs in reduced states. This is made possible by the relatively small energy differences between the strongly absorbing bands of LH2 (857 nm) and LH1 (880 nm). In LL B800 LH2 based on our models, the first low-energy excited state with significant dipole strength must lie somewhere in the region of 820–830 nm, with a consequent lower probability of energy back transfer. However, in our preparations not all B800–850 LH2 complexes are replaced by LL B800, and so the ability for back transfer of energy may be retained. Given that *Rps. palustris* grown at 90 lx contains ~15% B800–850 and we assume a photosystem model which has 8 or 9 LH2s to one LH1/RC complex (Papiz et al., 1997), then one or two B800–850 LH2s could be in contact with each LH1. Because energy moves rapidly ($<$100 fs) around B850 and B880 pigments, this could allow back energy transfer to the few B800–850 LH2s surrounding LH1. Alternatively, B800–850 may be exclusively part of an independent B800–850/LH1/RC domain (Nishimura et al., 1993) which begs the question: how can the B800–850 and B800 complexes organize into separate domains? The answer may lie in their different oligomeric symmetries. It has been suggested that the highly conserved charged residues, β-Asp(-13) and β-Arg(-10), found within the hydrophobic transmembrane domain, may be important in intercomplex assembly by forming salt bridges between complexes (Papiz et al., 1997). Some intercomplex assembly process may be necessary to keep the distances as small as possible to ensure efficient energy transfer. The disposition of these salt bridges may be sufficiently different between these two complexes to ensure that complexes with identical symmetries coalesce into mutually exclusive domains. There may also be a lag in the expression of different complexes linked to the changes in light intensity that encourages separate domain formation.

The question of whether energy is transferred in a delocalized state, or isolated on a B850 dimer from where a hopping mechanism is used to transport energy between neighboring dimers, has been debated in the literature (Bradforth et al., 1995; Visser et al., 1995; Pullerits et al., 1996; Chachisvilis et al., 1997; Monshouwer et al., 1997; Nagarajan et al., 1996; Meier et al., 1997; Leupold et al., 1996; Jimenez et al., 1997; Sundström et al., 1999; Novoderezhkin et al., 1999). This is a difficult question as the delocalized state seems to depend on the pigment-coupling energies, the time scale over which energy is reorganized, the magnitude of the disorder, and the temperature. It should also be noted that the physiological time scale of interest is

relatively short in LH2 (1–5 ps), and it is during this time scale that the energy states are changing very rapidly. Added to this is the difficulty of adequately formulating what constitutes a delocalized state. It is possible that this novel B800 complex can add something new to the discussion on this subject. Qy transition dipoles moments, aligned in a radial direction, have ~50% the interaction energy of those between B850 in B800–850 LH2. It might be expected then that localization would be more pronounced in B800 LH2. The possible involvement of more pigments complicates the matter further and more work is needed to assess this. However, if these extra pigments are present, then it may be expected that there are more interactions between pigments within a unit than between units, which could again add to energy localization on a repeating unit. Whatever the correct explanation for the origins of LL B800 spectra, it is clear that they differ substantially from those of B800–850, and this offers opportunities for comparative investigations which could resolve some of these issues. Ultimately, we wish to confirm the model with a high-resolution structure and perform detailed measurements and calculations of the spectroscopic properties of this novel complex.

Frank Sweeney and Hazel Tharia were supported by BBSRC grant nos. 719/B11638 and 719/B04960. We thank Dr. Sharon Kelly and Dr. Nick Price (BBSRC CD Facility, University of Glasgow) for help with the CD measurements and Daresbury Laboratory for supporting a number of university students.

REFERENCES

Alden, R. G., E. Johnson, V. Nagarajan, W. W. Parson, C. J. Law, and R. J. Cogdell. 1997. Calculation of spectroscopic properties of the LH2 bacteriochlorophyll protein antenna complex from *Rhodopseudomonas acidophila*. *J. Phys. Chem. B.* 101:4667–4680.

Bradforth, S. E., R. Jimenez, F. van Mourik, R. van Grondelle, and G. R. Fleming. 1995. Excitation transfer in the core light-harvesting complex (LH-1) of *Rhodobacter sphaeroides*: an ultra-fast fluorescence depolarization and annihilation study. *J. Phys. Chem.* 99:16719–16191.

Chachisvilis, M., O. Kühn, T. Pullerits, and V. Sundström. 1997. Excitons in photosynthetic purple bacteria. Wavelike motion or incoherent motion? *J. Phys. Chem. B.* 101:7275–7283.

Clayton, R. K. 1963. Absorption spectra, photosynthetic bacteria, and their chlorophylls. *In* Bacterial Photosynthesis. H. Gest, A. San Pietro and L. P. Vernon, editors. Antioch, Yellow Springs, OH. 495–500.

Collaborative Computational Project, Number 4 (CCP4). 1994. The CCP4 Suite: Programs for Protein Crystallography. *Acta Crystallogr. D.* 50: 760–763.

Cowtan, K. D., and P. Main. 1993. Improvement of macromolecular electron-density maps by the simultaneous application of real and reciprocal space constraints. *Acta Crystallogr. D.* 49:148–157.

Cupane, A., M. Leone, E. Vitrano, and L. Cordone. 1995. Low temperature optical absorption spectroscopy: an approach to the study of stereodynamic properties of hemeproteins. *Eur. Biophys. J.* 23:385–398.

Deinum, G., S. C. Otte, A. T. Gardiner, T. J. Aartsma, R. J. Cogdell, and J. Amesz. 1991. Antenna organization of *Rhodopseudomonas acidophila*: a study of excitation migration. *Biochim. Biophys. Acta.* 1060:125–131.

Evans, M. B. 1989. The structure and function of antenna complexes of purple photosynthetic bacteria. Ph.D. thesis. University of Glasgow, Scotland. 1–220.

Evans, M. B., A. M. Hawthornthwaite, and R. J. Cogdell. 1990. Isolation and characterisation of different B800–850 light-harvesting complexes from low- and high-light grown cells of *Rhodopseudomonas palustris*, strain 2.1.6. *Biochim. Biophys. Acta.* 1016:71–76.

Fowler, G. J., G. D. Sockalingum, B. Robert, and C. N. Hunter. 1994. Blue-shifts in bacteriochlorophyll absorbance correlate with changed hydrogen bonding patterns in light-harvesting LH2 mutants of *Rhodobacter sphaeroides* with alterations at α-Tyr44 and 45. *Biochem. J.* 299:695–700.

Fowler, G. J., R. W. Visschers, G. G. Grief, R. van Grondelle, and C. N. Hunter. 1992. Genetically modified photosynthetic antenna complexes with blue-shifted absorbance bands. *Nature.* 355:695–700.

Freer, A., S. Prince, K. Sauer, M. Papiz, A. Hawthornthwaite-Lawless, G. McDermott, R. Cogdell, and N. W. Isaacs. 1996. Pigment-pigment interactions and energy transfer in the antenna complex of the photosynthetic bacterium *Rhodopseudomonas acidophila*. *Structure*. 4:449–462.

Freiberg, A., J. P. Allen, J. C. Williams, and N. W. Woodbury. 1996. Energy trapping and detrapping by wild type and mutant reaction centers of purple non-sulfur bacteria. *Photosynth. Res.* 48:309–319.

Gall, A., and B. Robert. 1999. Characterization of the different peripheral light-harvesting complexes from high- and low-light grown cells from *Rhodopseudomonas palustris. Biochemistry.* 38:5185–5190.

Gardiner, A. T., R. J. Cogdell, and S. Takaichi. 1993. The effect of growth conditions on the light-harvesting apparatus in *Rhodopseudomonas acidophila. Photosynth. Res.* 38:159–167.

Hawthornthwaite, A. M., and R. J. Cogdell. 1991. The Chlorophylls. H. Scheer, editor. CRC Press, Boca Raton. 493–528.

Hess, S., M. Chachisvilis, K. Timpmann, M. R. Jones, G. J. Fowler, C. N. Hunter, and V. Sundström. 1995. Temporally and spectrally resolved sub-picosecond energy transfer within LH2 and from LH2 to LH1 in photosynthetic purple bacteria. *Proc. Natl. Acad. Sci. U.S.A.* 92: 12333–12337.

Jimenez, R., S. N. Dikshit, S. E. Bradforth, and G. R. Fleming. 1996. Electronic excitation transfer in the LH2 complex of *Rhodobacter sphaeroides. J. Phys. Chem.* 100:2399–2409.

Jimenez, R., F. van Mourik, and G. R. Fleming. 1997. Three pulse echo peak shift measurements on LH1 and LH2 complexes of *Rhodobacter sphaeroides*: a nonlinear spectroscopic probe of energy transfer. *J. Phys. Chem. B.* 101:7350–7359.

Jones, T. A., J. Y. Zou, S. W. Cowan, and M. Kjeldgaard. 1991. Improved method for binding protein models in electron density maps and the location of errors in these models. *Acta Crystallogr. A.* 47:110–119.

Karrasch, S., P. A. Bullough, and R. Ghosh. 1995. The 8.5 Å projection map of the light-harvesting complex I from *Rhodospirillum rubrum* reveals a ring composed of 16 subunits. *EMBO J.* 14:631–638.

Kerfeld, C. A., T. O. Yeates, and J. P. Thornber. 1994. Purification and characterisation of the peripheral antenna of the purple non-sulfur bacterium *Chromatium purpuratum*: evidence of an unusual pigment-protein composition. *Biochemistry.* 33:2178–2184.

Kissinger, C. R., D. K. Gehlhaar, and D. Fogel. 1999. Rapid automated molecular replacement by evolutionary search. *Acta Crystallogr. D.* 55:484–491.

Koepke, J., X. Hu, C. Muenke, K. Schulten, and H. Michel. 1996. The crystal structure of the light-harvesting complex II (B800–850) from *Rhodospirillum molischianum. Structure.* 4:581–597.

Koolhaas, M. H., R. N. Frese, G. J. Fowler, T. S. Bibby, S. Georgakopoulou, G. van der Zwan, C. N. Hunter, and R. van Grondelle. 1998. Identification of the upper exciton component of the B850 bacteriochlorophylls of the LH2 complex, using a B800-free mutant of *Rhodobacter sphaeroides*. *Biochemistry.* 37:4693–4698.

Koolhaas, M. H., G. van der Zwan, R. N. Frese, and R. van Grondelle. 1997. Red-shift of the zero crossing in the CD spectra of the LH2 antenna complex of *Rhodopseudomonas acidophila*: a structure based study. *J. Phys. Chem. B.* 101:7262–7270.

Krueger, B. P., G. D. Scholes, and G. R. Fleming. 1998. Calculation of couplings and energy-transfer pathways between the pigments of LH2 by the ab initio Transition Density Cube method. *J. Phys. Chem. B.* 102:5378–5386.

Leegwater, J. A. 1996. Coherent versus incoherent energy transfer and trapping in photosynthetic antenna complexes. *J. Phys. Chem.* 100: 14403–14409.

Leslie, A. G. 1990. Crystallographic Computing. Oxford University Press, New York.

Leupold, D., H. Stiel, K. Teuchner, F. Nowak, W. Sander, B. Ucker, and H. Scheer. 1996. Size enhancement of transition dipoles to one and two-exciton bands in photosynthetic antenna. *Phys. Rev. Lett.* 77: 4675–4678.

Ma, Y. Z. 1998. Excitation energy transfer in purple and green photosynthetic bacteria. Ph.D. thesis. University of Umeå, Sweden. 1–157.

McDermott, G., S. M. Prince, A. A. Freer, A. M. Hawthornthwaite-Lawless, M. Z. Papiz, R. J. Cogdell, and N. W. Isaacs. 1995. Crystal structure of an integral membrane light-harvesting complex from photosynthetic bacteria. *Nature.* 374:517–512.

McLuskey, K., S. M. Prince, R. J. Cogdell, and N. W. Isaacs. 1999. Crystallization and preliminary X-ray crystallographic analysis of the B800–820 light-harvesting complex from *Rhodopseudomonas acidophila* strain 7050. *Acta Crystallogr. D.* 55:885–887.

Meier, T., V. Chernyak, and S. Mukamel. 1997. Multiple exciton coherence sizes in photosynthetic antenna complexes viewed by pump probe spectroscopy. *J. Phys. Chem. B.* 101:7332–7342.

Monshouwer, R., M. Abrahamson, F. van Mourik, and R. van Grondelle. 1997. Superradiance and exciton delocalisation in bacterial photosynthetic light-harvesting systems. *J. Phys. Chem. B.* 101:7241–7248.

Monshouwer, R., I. Ortiz de Zarate, F. van Mourik, and R. van Grondelle. 1995. Low-intensity pump-probe spectroscopy on the B800 to B850 transfer in the light harvesting 2 complex of *Rhodobacter sphaeroides. Chem. Phys. Lett.* 246:341–346.

Nagarajan, V., R. G. Alden, J. C. Williams, and W. W. Parson. 1996. Ultrafast exciton relaxation in the B850 antenna complex of *Rhodobacter sphaeroides*. *Proc. Natl. Acad. Sci. U.S.A.* 93: 13774–13779.

Nagarajan, V., and W. W. Parson. 1997. Excitation energy transfer between the B850 and B875 antenna complexes of *Rhodobacter sphaeroides. Biochemistry.* 36:2300–2306.

Nishimura, Y., K. Shimada, I. Yamazaki, and M. Mimuro. 1993. Energy transfer processes in *Rhodopseudomonas palustris* grown under low-light conditions: heterogeneous composition of LH2 complexes and parallel energy flow pathways. *FEBS Lett.* 329:319–323.

Novoderezhkin, V., R. Monshouwer, and R. van Grondelle. 1999. Exciton delocalization in the LH2. antenna of *Rhodobacter sphaeroides* as revealed by relative difference absorption of the LH2 antenna and the B820 subunit. *J. Phys. Chem. B.* 103:10540–10548.

Papiz, M. Z., S. M. Prince, A. M. Hawthornthwaite-Lawless, G. McDermott, A. A. Freer, N. W. Isaacs, and R. J. Cogdell. 1997. A model for the photosynthetic apparatus of purple bacteria. *Trends Plant Sci.* 1:198–206.

Philipson, K. D., D. Cheng Tsai, and K. Sauer. 1971. Circular dichroism of chlorophyll and related molecules calculated using a point monopole model for the electronic transitions. *J. Phys. Chem.* 75:1440–1445.

Pullerits, T., M. Chachisvilis, and V. Sundström. 1996. Exciton delocalization length in the B850 antenna of *Rhodobacter sphaeroides. J. Phys. Chem.* 100:10787–10792.

Sauer, K., R. J. Cogdell, S. M. Prince, A. A. Freer, N. W. Isaacs, and H. Scheer. 1996. Structure-based calculations of the optical spectra of the LH2 bacteriochlorophyll protein complex from *Rhodopseudomonas acidophila. Photochem. Photobiol.* 64:564–576.

Sturgis, J. N., V. Jirsakova, F. Reiss-Husson, R. J. Cogdell, and B. Robert. 1995. Structure and properties of the bacteriochlorophyll binding-site in peripheral light-harvesting complexes of purple bacteria. *Biochemistry.* 34:517–523.

Sundström, V., T. Pullerits, and R. van Grondelle. 1999. Photosynthetic light-harvesting: reconciling dynamics and structure of purple bacterial LH2 reveals function of photosynthetic unit. *J. Phys. Chem. B.* 103: 2327–2346.

Tadros, M. H., E. Katsiou, M. A. Hoon, N. Yurkova, and D. P. Ramji. 1993. Cloning of a new antenna gene cluster and expression analysis of the antenna gene family of *Rhodopseudomonas palustris. Eur. J. Biochem.* 217:867–875.

Tharia, H. A., T. D. Nightingale, M. Z. Papiz, and A. M. Lawless. 1999. Characterisation of hydrophobic peptides by RP-HPLC from different spectral forms of LH2 isolated from *Rhodopseudomonas palustris. Photosynth. Res.* 61:157–157.

Timpmann, K., A. Freiberg, and V. Sundström. 1995. Energy trapping and detrapping in photosynthetic bacteria *Rhodopseudomonas viridis. Chem. Phys.* 194:275–283.

Vagin, A. A., and A. Teplyakov. 1997. MOLREP: an automated program for molecular replacement. *J. Appl. Crystallogr.* 30:1022–1025.

van Mourik, F., A. M. Hawthornthwaite, C. Vonk, M. B. Evans, R. J. Cogdell, V. Sundström, and R. van Grondelle. 1992. Spectroscopic characterisation of the low-light B800–850 light-harvesting complex of *Rhodopseudomonas palustris,* strain 2.1.6. *Biochim. Biophys. Acta.* 1140:85–93.

Vila, X., J. Colomer, and L. J. Garcia-Gil. 1996. Modelling spectral irradiance in freshwater in relation to phytoplankton and solar radiation. *Ecol. Model.* 87:59–68.

Visscher, K. J., H. Bergström, V. Sundström, C. N. Hunter, and R. van Grondelle. 1989. Temperature dependence of energy transfer from the long wavelength antenna BChl-896 to the reaction center in *Rhodospirillum rubrum, Rhodobacter sphaeroides* (w.t. and M21 mutant) from 77 to 177 K, studied by picosecond absorption spectroscopy. *Photosynth. Res.* 22:211–217.

Visser, H. M., O. J. Somsen, F. van Mourik, S. Lin, I. H. van Stokkum, and R. van Grondelle. 1995. Direct observation of sub-picosecond equilibration of excitation energy in the light-harvesting antenna of *Rhodospirillum rubrum. Biophys. J.* 69:1083–1099.

Weiss, Jr., C. 1972. The π electron structure and absorption spectra of chlorophylls in solution. *J. Mol. Spec.* 44:37–80.

Zhang, F. G., R. van Grondelle, and V. Sundström. 1992. Pathways of energy flow through the light-harvesting antenna of the photosynthetic purple bacterium *Rhodobacter sphaeroides. Biophys. J.* 61:911–920.

Zuber, H., and R. A. Brunisholz. 1991. The Chlorophylls. H. Scheer, editor. CRC Press, Boca Raton. 627.